

UNCLASSIFIED

|   |  |
|---|--|
| AD NUMBER   |  |
| ADA074622   |  |
| CLASSIFICATION CHANGES                                      |  |
| TO:   | UNCLASSIFIED   |
| FROM:   | CONFIDENTIAL   |
| LIMITATION CHANGES  |  |
| TO:   | Approved for public release; distribution is unlimited.  |
| FROM:   | Distribution authorized to DoD only; Administrative/Operational Use; MAR 1954. Other requests shall be referred to Atomic Energy Commission, Washington, DC. Pre-dates formal DoD distribution statements. Treat as DoD only. Restricted Data. |
| AUTHORITY   |  |
| DSWA/OPSSI ltr dtd 8 May 1998 DSWA/OPSSI ltr dtd 8 May 1998 |  |

THIS PAGE IS UNCLASSIFIED

ADA074622

ACCESSION NUMBER



**LEVEL**

## DATA PROCESSING SHEET

**PHOTOGRAPH THIS SHEET**



## **INVENTORY**

AEC WT-740

**DOCUMENT IDENTIFICATION**

**DISTRIBUTION STATEMENT A**

Approved for public release;  
Distribution Unlimited

**DISTRIBUTION STATEMENT**

Accession For  
NTIS GRA&I  
DDC TAB  
Unannounced  
Justification 

---

By Per Hs. on file

---

Distribution /

---

Availability Codes

---

| Dist. | Avail and/or<br>special |
|-------|-------------------------|
| A     |                         |

**DISTRIBUTION STAMP**

D D C  
RECORDED  
OCT 3 1979  
D

**DATE ACCESSIONED**

70 10 01 123

DATE RECEIVED IN DDC

**PHOTOGRAPH THIS SHEET**

AND RETURN TO DDA-2

AD A 074622

~~CONFIDENTIAL~~ UNCLASSIFIED

019087  
WT-740

Copy No. 172 A

319-1 C 172A

TECHNICAL LIBRARY  
 of the  
DEFENSE NUCLEAR  
AGENCY

AUG 1 1974

# Operation UPSHOT-KNOTHOLE

NEVADA PROVING GROUNDS

March - June 1953

Project 3.26.5

PRESSURE MEASUREMENTS ON STRUCTURES

RECORDED UNCLASSIFIED

BY AUTHORITY OF DP. FORM 15.75 <sup>17424</sup> 1000/2 1716 Aug 63  
BY B. W. W. 23 Sep 64

~~RESTRICTED DATA~~

This document contains restricted data as  
defined in the Atomic Energy Act of 1946.  
Its transmission, communication, disclosure or its  
contents in any manner to an unauthorized



HEADQUARTERS FIELD COMMAND, ARMED FORCES SPECIAL WEAPONS PROJECT  
SAN JUAN BASE, ALBUQUERQUE, NEW MEXICO

UNCLASSIFIED

~~CONFIDENTIAL~~

If this report is no longer needed, return it to  
ABC Technical Information Service  
P. O. Box 601  
Oak Ridge, Tennessee

~~CONFIDENTIAL~~ UNCLASSIFIED

WT-740

This document consists of 44 pages  
No. 172 of 270 copies, Series A

OPERATION UPHOT-KNOTHOLE

Project 3.28.3

PRESSURE MEASUREMENTS ON STRUCTURES

REPORT TO THE TEST DIRECTOR

by

L. M. Swift

RECORDED

UNCLASSIFIED

BY AUTHORITY OF DA FORM 1575 274/24  
BY B. Wade 23 SEP 64 11/6 Aug 63

March 1954

~~RESTRICTED DATA~~

This document contains restricted data as  
defined in the Atomic Energy Act of 1946.  
Its transmission or the disclosure of its  
content in any manner to an unauthorized  
person is prohibited

Stanford Research Institute  
Palo Alto, California

~~CONFIDENTIAL~~

UNCLASSIFIED

UNCLASSIFIED

ABSTRACT

Project 3.28.3 of Operation UPSHOT-KNOTHOLE was concerned with the measurement of pressures existing on the surfaces of various non-responsive structures from Shots 9 and 10. The experiment plan and the analysis of data were not a portion of this project, but the data will be used in computation of structural loading and response under air blast. A secondary portion of the project was the definition of air blast conditions existing at the time of measurement.

A total of 143 satisfactory records were obtained from the two shots, a 99.3 per cent performance. Secondary air blast records were analyzed and the results are included for the use of other projects.

per telecon w/Betty Fox (DNA Tech Libr, Chief), the  
classified references contained herein may remain.

*J. C. Lachance (DDIA-2)*  
9-5-79

UNCLASSIFIED

UNCLASSIFIED

FOREWORD

This report is one of the reports presenting the results of the 78 projects participating in the Military Effects Tests Program of Operation UPSHOT-KNOTHOLE, which included 11 test detonations. For readers interested in other pertinent test information, reference is made to WT-782, Summary Report of the Technical Director, Military Effects Program. This summary report includes the following information of possible general interest.

- a. An over-all description of each detonation, including yield, height of burst, ground zero location, time of detonation, ambient atmospheric conditions at detonation, etc., for the 11 shots.
- b. Compilation and correlation of all project results on the basic measurements of blast and shock, thermal radiation, and nuclear radiation.
- c. Compilation and correlation of the various project results on weapons effects.
- d. A summary of each project, including objectives and results.
- e. A complete listing of all reports covering the Military Effects Tests Program.

UNCLASSIFIED

UNCLASSIFIED

PREFACE

This report presents the results of air pressure vs time measurements made on the surface of certain non-responsive structures, and also similar measurements made at or near the surface of the ground in the general vicinity of these structures, on two nuclear explosions of Operation UPSHOT-KNOTHOLE.

Tracings and tabulations of all the above records were made and distributed prior to the completion of this part of the report.<sup>1/</sup> Therefore, this report is physically in three parts: (1) the material contained in this binder; (2) a binder containing the tracings of the original records (Appendix A); and (3) another binder containing the calibrations and tabulated pressure-time data (Appendix B). Appendices A and B are available at the Stanford Research Institute.

<sup>1/</sup> All numbered references refer to the Bibliography at the end of this report.

UNCLASSIFIED

CONTENTS

|                                    |    |
|------------------------------------|----|
| ABSTRACT.....                      | 3  |
| FOREWORD.....                      | 5  |
| PREFACE.....                       | 7  |
| ILLUSTRATIONS.....                 | 11 |
| TABLES.....                        | 11 |
| CHAPTER 1 INTRODUCTION.....        | 13 |
| 1.1 Objectives.....                | 13 |
| 1.2 Scope.....                     | 13 |
| CHAPTER 2 EXPERIMENT DESIGN.....   | 14 |
| 2.1 Predictions.....               | 14 |
| 2.2 Gage Layout.....               | 14 |
| 2.2.1 Gages on Structures.....     | 14 |
| 2.2.2 Free-Field Gages.....        | 14 |
| 2.2.3 Gage Coding.....             | 18 |
| CHAPTER 3 INSTRUMENTATION.....     | 19 |
| 3.1 General Instrument System..... | 19 |
| 3.2 Gages.....                     | 19 |
| 3.3 Station Equipment.....         | 20 |
| 3.4 Calibration Procedure.....     | 21 |
| 3.5 Over-all Characteristics.....  | 21 |
| CHAPTER 4 RECORD ANALYSIS.....     | 22 |
| CHAPTER 5 RESULTS.....             | 24 |
| 5.1 General.....                   | 24 |
| 5.2 Structural Measurements.....   | 24 |

|                                    |    |
|------------------------------------|----|
| 5.3 Free-Field Measurements.....   | 24 |
| 5.3.1 Side-On Pressure.....        | 24 |
| 5.3.2 Effect of Stabilization..... | 33 |
| 5.3.3 Diffraction Effects.....     | 38 |
| CHAPTER 6 CONCLUSIONS.....         | 39 |
| 6.1 Structural Measurements.....   | 39 |
| 6.2 Free-Field Measurements.....   | 39 |
| BIBLIOGRAPHY.....                  | 41 |

ILLUSTRATIONS

|  |    |
|--|----|
| 2.1 Layout of Structures and Free-Field Gages.....             | 17 |
| 4.1 Typical Calibration Curve.....                             | 23 |
| 5.1 Comparison of SRI and BRL Records.....                     | 25 |
| 5.2 Free-Field Records - Shot 9.....                           | 27 |
| 5.3 Fitting Free-Field Records to Idealized Curve-Shot 9.....  | 30 |
| 5.4 Average Side-On Pressure Curve - Shot 9.....               | 32 |
| 5.5 Free-Field Records - Shot 10.....                          | 34 |
| 5.6 Fitting Free-Field Records to Idealized Curve-Shot 10..... | 35 |
| 5.7 Average Side-On Pressure - Shot 10.....                    | 36 |
| 5.8 Gage BI Records - Shots 9 and 10.....                      | 37 |

TABLES

|  |       |
|--|-------|
| 2.1 Gage Locations on Structures - Shots 9 and 10..... | 15,16 |
| 5.1 Comparison of SRI and BRL Results.....             | 26    |
| 5.2 Summary of Free-Field Measurements.....            | 28    |
| 5.3 Results of Curve Fittings.....                     | 31    |

~~CONFIDENTIAL~~

~~UNCLASSIFIED~~

## CHAPTER 1

### INTRODUCTION

#### 1.1 OBJECTIVES

The primary objective of this project was to make pressure-time measurements on several structures of Project 3.1 and report the resulting data in a form suitable for coordination with similar data from other agencies.

Since validity of calculations based on these data is largely dependent upon the accurate determination of the pressure-time conditions to which the targets were subjected, it was considered desirable to obtain reliable measurements which would describe these "side-on" pressures. This became a secondary objective of this project. Another secondary objective was to determine, if possible, the effect on the blast wave of the stabilization of the ground surface around the structures.

#### 1.2 SCOPE

Stanford Research Institute (SRI) shared with the Ballistic Research Laboratories (BRL) and the Naval Ordnance Laboratory (NOL) the responsibility for the instrumentation of the structures of Project 3.1. This responsibility did not include the basic planning of the experiment or the analysis and interpretation of the results. Other agencies were assigned these tasks. A partial exception was the study of free-field measurements. The analysis of these data and their application to the structural measurements was considered to be primarily a responsibility of this project, insofar as the 3.1 structures located at a radius of 4900 ft were concerned. On this project a total of 78 gages were installed on each shot (Shots 9 and 10), 54 on 3.1 structures, and 24 apart from the structures to measure free-field conditions.

~~CONFIDENTIAL~~

~~RESTRICTED DATA~~

~~UNCLASSIFIED~~

## CHAPTER 2

### EXPERIMENT DESIGN

#### 2.1 PREDICTIONS

In the design of the experimental measurements on structures, predictions of average peak pressures on the surface of each target were presumably based largely on the prediction methods developed for, and modified by experience in, Operation GREENHOUSE<sup>2</sup> and on the pretest studies.<sup>3</sup> The "side-on" peak pressures to be expected on each shot were taken from composite curves formed by scaling and interpolation of data from Operation TUMBLER<sup>4</sup> and previous nuclear tests.

#### 2.2 GAGE LAYOUT

##### 2.2.1 Gages on Structures

Gages were located on the structures as listed in Table 2.1. The locations shown are for reference only; the actual locations are shown in the summary report of Project 3.1.<sup>5</sup> In the cases of Structures 3.1-c, -d, -f, -i, -m, -n, and -q, the measurements were primary in that this project was assigned the full responsibility for the measurements on these structures. It will be observed that although 54 gage positions are shown on these structures they represent a total of only 48 gage channels, since on each of two channels on Structure 3.1-m four gages were connected to a single channel in such a fashion as to measure the average pressure. In addition to these primary gages, a few gages were located on Structures 3.1-a, -e, and -g alongside gages of the Ballistic Research Laboratories (Project 3.28.1) for the purpose of comparison of the two types of instrumentation.

##### 2.2.2 Free-Field Gages

The Project 3.1 structures at a 4900-ft radius were arranged in an arc subtending an angle of over 20 degrees around the instrument ground zero. All calculations and predictions assumed that the blast wave would be identical at all targets. However, due to the possibility of blast wave asymmetry at ground level, and the fact that true

Table 2.1 - Gage Locations on Structures - Shots 9 and 10

| Structure | Structure Dimensions* (ft) | Gage  | Location                                       | Feet From Top   | Feet From Left Side**  | Feet From Front          |
|-----------|----------------------------|---|--|---|--|--------------------------|
| 3.1a      | 6x12x6                     | P1<br>P6<br>P8<br>P17                                     | F<br>F<br>R<br>R                               | 1.0<br>4.5<br>1.0<br>4.5                              | 6.0<br>6.0<br>1.0<br>6.0   |                          |
| 3.1c      | 6x6x6                      | P1<br>P2<br>P3<br>P4<br>P5<br>P6<br>P7<br>P8<br>P9<br>P10 | T<br>T<br>T<br>T<br>F<br>F<br>R<br>R<br>R<br>R |   | 3.0<br>1.0<br>3.0<br>1.0<br>1.0<br>3.0<br>1.0<br>1.0<br>1.0<br>3.0 | 5.0<br>5.0<br>1.0<br>1.0 |
| 3.1d      | 6x12x1                     | P1<br>P2<br>P3<br>P4<br>P5<br>P6<br>P7<br>P8              | R<br>R<br>R<br>R<br>R<br>F<br>F<br>F           | 1.0<br>1.0<br>2.75<br>4.5<br>4.5<br>1.0<br>1.0<br>4.5 | 1.0<br>6.0<br>3.5<br>1.0<br>6.0<br>6.0<br>1.0<br>6.0               |                          |
| 3.1e      | 18x36x18                   | P5  | R  | 3.0   | 18.0   |                          |
| 3.1f      | 12x24x12                   | P1<br>P2<br>P3<br>P4<br>P5                                | T<br>T<br>F<br>R<br>T                          |   | 12.0<br>12.0<br>12.0<br>12.0<br>12.0                               | 2.0<br>1.0               |
| 3.1g      | 6x12x6                     | P1(B)<br>P7(A)<br>P11<br>P15                              | F<br>R<br>LS<br>RS                             | 1.0<br>3.0<br>2.75<br>2.75                            | 6.0<br>6.0   | 3.0<br>3.0               |

\* - Dimensions given in order of height, width, and length  
 \*\* - Left and right sides defined as viewed from rear

Table 2.1(conc.) - Gage Locations on Structures - Shots 9 and 10

| Structure | Structure Dimensions*<br>(ft)                   | Gage  | Location  | Feet<br>From<br>Top   | Feet<br>From<br>Left Side**  | Feet<br>From<br>Front |
|-----------|---|---|---|---|--|-----------------------|
| 3.li      | 6x12x18   | P1<br>P2<br>P3<br>P4<br>P5<br>P6                                  | T<br>R<br>R<br>R<br>R<br>R  | 1.0<br>1.0<br>1.0<br>3.0<br>4.5<br>4.5                                    | 6.0<br>1.0<br>6.0<br>3.5<br>1.0<br>6.0                                   | 3.0                   |
| 3.lm      | 6x12x8<br>(Two slabs<br>6' apart<br>1' thick)   | P1<br>P2<br>P3<br>P4<br>P5<br>P6                                  | Ground<br>R(2)<br>F(2)<br>F(2)<br>R(1)<br>R(1)                              | 1.0<br>Av.<br>4.5<br>Av.<br>3.5   | 6.0<br>6.0<br>Av.<br>6.0<br>Av.<br>6.0                                   | 4.0                   |
| 3.ln      | 6x12x20<br>(Two slabs<br>18' apart<br>1' thick) | P1<br>P2  | F(2)<br>R(1)  | 4.5<br>4.5  | 6.0<br>6.0   |                       |
| 3.lq      | 10x6x11<br>(Reentrant<br>structure)             | P1<br>P2<br>P3<br>P4<br>P5<br>P6<br>P7<br>P8<br>P10<br>P11<br>P12 | F(3)<br>F(3)<br>F(3)<br>R(1)<br>F(2)<br>F(2)<br>F(2)<br>RS<br>RS<br>RS<br>F | 1.0<br>1.0<br>4.5<br>1.0<br>1.0<br>2.0<br>4.5<br>1.0<br>4.5<br>3.0<br>3.0 | 1.25<br>2.33<br>2.33<br>1.25<br>0.5<br>0.5<br>0.5<br>9.25<br>9.25<br>1.5 |                       |

\* - Dimensions given in order of height, width, and length

\*\* - Left and right sides defined as viewed from rear

NOTE: Dimensions given are from design drawings. As-built dimensions vary slightly from these.

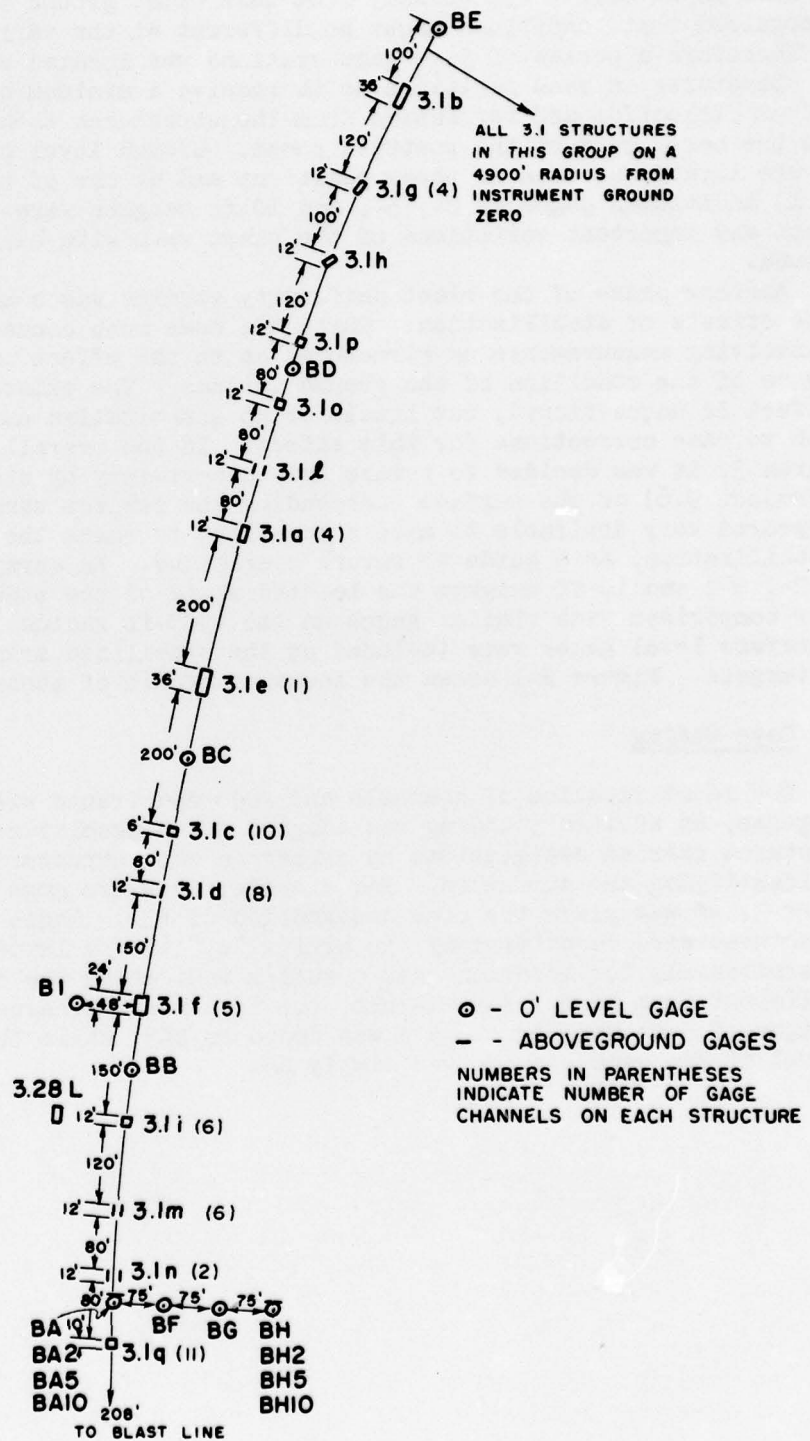


Fig. 2.1 Layout of Structures and Free-Field Gages

ground zero might differ appreciably from instrument ground zero, it was recognized that conditions might be different at the various targets. Therefore a series of five gage stations was located along the arc of structures in such positions as to receive a minimum of disturbance from reflection and refraction from the structures themselves--none in the early part of the positive phase. Ground level pressure gages were located at each of these positions and at one of them (BA, Fig. 2.1) additional gages at 2-, 5-, and 10-ft heights were installed to detect any important variations of the blast wave with height above the ground.

Another phase of the blast uniformity studies was concerned with the effects of stabilization. There has been much concern in all tests involving measurements on structures as to the effect on the blast wave of the condition of the ground surface. The existence of this effect is unquestioned, but little or no quantitative data existed on which to base corrections for this effect. In the overall planning of Program 3, it was decided to reduce this uncertainty by stabilization (Project 9.6) of the surface surrounding the subject targets. It then appeared very desirable to make some effort to check the effect of this stabilization, as a guide to future operations. An array of gages at 0-, 2-, 5-, and 10-ft heights was located ahead of the stabilized area for comparison with similar gages on the 4900-ft radius. Two other surface level gages were included on the stabilized area ahead of the targets. Figure 2.1 shows the location of all of these gages.

### 2.2.3 Gage Coding

For identification of channels and recorded traces with their proper gages, an arbitrary coding was adopted for nomenclature. Gages on structures carried designations by number on each structure, and a letter identifying the structure. For example, pressure gage no. 3 on Structure 3.1-f was given the code designation of P3F. Gages not on the structures were identified by the prefix "B," then a letter assigned arbitrarily for location, and a suffix indicating the height when different from zero. For example, the free-field pressure gage at a height of 5 ft at Structure A was coded as BA5, while the one at zero level at the same station was simply BA.

## CHAPTER 3

### INSTRUMENTATION

#### 3.1 GENERAL INSTRUMENT SYSTEM

All channels of instrumentation were essentially identical to those described in previous reports.<sup>6,7</sup> Wiancko balanced variable reluctance pressure transducers were connected through modified Wiancko station equipment to William Miller Co. oscillograph recorders. The final records were produced on 12-in. photographic paper, the exposed records being recovered within 12 hours after each shot and processed at once. This system had been proven satisfactory by use in a number of previous operations, its simplicity and reliability being its outstanding features.

The recording instrumentation was located in an underground shelter, 3.28L, immediately behind the line of target structures (Fig. 2.1). The concrete walls of this shelter, in addition to a few feet of covering earth, were designed to provide ample shielding from radiation to prevent any fogging of the sensitive recording paper. All instrumentation was unmanned during each shot.

#### 3.2 GAGES

The gages used on this operation were the Wiancko type 3PAD. In this type of gage two coils are used connected in a "half-bridge" circuit. Pressure applied to the twisted tube sensing element displaces the armature in such a fashion as to change the inductance of the two coils in opposite directions, thereby unbalancing the bridge. This construction provides a high degree of freedom from spurious excitation due to acceleration and temperature effects.

The undamped natural frequency of the gages used ranged from 1400 to 1800 cps. Damping provisions in these instruments require the use of a semi-fluid silicone grease in a narrow gap between the moving armature and a fixed damping plate. This type of damping had been found to be somewhat non-linear. If an attempt were made to damp the gage response sufficiently to eliminate ringing it was found that the later portion of the rise time showed seriously over-damped characteristics requiring several milliseconds to reach a final value. This

behavior would result in the "rounding" of the peak of a recorded pressure wave. In order to avoid this very undesirable characteristic, the damping in each gage was reduced to a point where the full initial rise time was less than 0.5 msec even though this resulted in severe overshoot and ringing, when viewed with full frequency resolution.

### 3.3 STATION EQUIPMENT

The gages were connected to the equipment in the recording shelter through 3-conductor shielded flexible cable buried where necessary to avoid damage from traffic and from the blast wave. A carrier voltage of approximately 20 volts at 3000 cps was supplied to each gage from a Wiancko type 3EP12 carrier oscillator. Each oscillator supplied power to 12 gages and their associated conversion equipment. The six oscillators used in this station were locked together in frequency and phase by an added locking circuit, to avoid any undesirable beats which might be caused by small differences in frequency between oscillators. This circuit was so arranged that, although one oscillator was used as the "master" to determine the frequency of all others, if this master failed the remaining oscillators would continue to provide output at practically their full normal voltage.

The conversion equipment used in this system did not include any vacuum tube amplifiers. The signal output of the gages was of sufficient magnitude to drive the recording galvanometers directly after demodulation. Each channel included an attenuator for regulating the recorded amplitude and a balancing control for setting the steady-state output to zero. Provisions were also included for manually or automatically injecting a calibrating voltage into the circuit to provide a synthetic "calibration signal" of controlled magnitude.

The recording galvanometers used in this operation were all of an undamped natural frequency of 315 to 340 cps. Damping resistors were adjusted to provide a damping factor of 0.6 to 0.7. The frequency response of these galvanometers was such that the "ringing" frequency of the gages described in section 3.2 was almost completely eliminated on the final record. The response time of the over-all recording system was determined almost entirely by the characteristics of the recording galvanometers.

Although each recording oscilloscope incorporated a timing system which impressed timing lines on the final record at 10 millisecond intervals, it had been found in previous operations that the precision of relative timing between recorders was not entirely satisfactory. In order to provide highly accurate absolute and relative timing, a crystal controlled secondary frequency standard was used. From this standard, signal voltages of 1000 and 100 cps were recorded by galvanometers on each recorder. Since these signals were supplied from a common source, the resultant time markers were identical on all records and essentially perfect time correlation between records could be obtained.

The prime power supply for instruments during shots was a bank of storage batteries. Suitable converters were used to produce 115 volts AC for such components as required this type of source. Instruments were powered at suitable times before zero time by Edgerton, Germeshausen and Grier (EG&G) relay circuits, with lock-in relays controlled

by a time delay relay to continue operation for approximately 1 minute after zero time in spite of the fact that the EG&G relays dropped out sooner. Utmost attention was paid to circuitry and procedures to insure maximum reliability of operation. Dual relay contacts or dual relays were used wherever feasible. A multi-pen recorder was connected to provide a record of operating time and sequence of various elements, so that any failure might be traced to its source in a post-test study.

### 3.4 CALIBRATION PROCEDURE

Calibration was performed after all gages had been installed in their final location and connected to their respective channels for each shot. After each shot, a postshot calibration was performed to check the stability of the system.

In the calibration procedure several pressures ranging from zero to approximately 150 per cent of the expected peak pressure were applied to the gage in sequence. These pressure values were read with a mercury manometer or a laboratory dial gage whose calibration was checked frequently with a dead weight tester. For each pressure the actual galvanometer deflection was noted and recorded. In addition, the deflection caused by the synthetic "calibration signal" was recorded. All attenuator and calibration signal voltage settings were recorded and rechecked immediately prior to leaving the station before each shot. This procedure provided the maximum of assurance that conditions were unchanged between the time of calibration and the actual shot. During the final record, about 10 sec before zero time, the calibration signals were impressed on each channel in succession.

### 3.5 OVER-ALL CHARACTERISTICS

As stated in section 3.3, the response time of the gage recording system was determined by the characteristics of the recording galvanometers. Calculations confirmed by actual measurements on records taken of HE blast waves with these gages and recording circuits show a rise time (to 90 per cent peak amplitude) of 1.3 msec. It may be concluded then that a record showing rise times of over 1.5 msec may be considered to indicate blast wave conditions other than a pure shock wave.

Calibration pressures and their corresponding galvanometer deflections were read to an accuracy of approximately 2 per cent of the expected peaks. Repeated calibrations over a considerable time showed a maximum change of calibration of 4 per cent, the average being considerably lower.

## CHAPTER 4

### RECORD ANALYSIS

As soon as possible after each shot, the records were recovered and processed. Certain preliminary readings and tracings were made in the field for inclusion in the preliminary report. These readings and calculations were ignored in the final analysis of the data.

The first step in establishing the calibration factors used in the final reading of the records was to read the deflections on the final records caused by the automatically impressed calibration signals. The ratio between these readings and the manual readings of the same deflection taken at the time of calibration was used to correct the calibration figures taken at the time of calibration (this ratio was seldom greater than 1.03). The combined calibration data thus corrected for both the pretest and post-test field calibration were used to establish the calibration curve for each gage record. When these points were plotted on coordinates of deflection vs. pressure it was found that although there was some indication of non-linearity it was very slight over the deflection ranges involved. Statistically speaking the probable deviation from the best curve drawn through the data points was only a small fraction of 1 per cent lower than the probable deviation from the best straight line drawn through these points. Consequently, it was decided that the probable error caused by using a straight line calibration curve would be imperceptibly higher than that caused by using a curved calibration curve, and linear calibrations were used in reading the records for the final data presentation. Figure 4.1 shows a typical calibration curve.

On each record the true zero time was indicated by a small temporary displacement of the trace caused by the induction signal. The records were counted out from this fiducial marker using the high accuracy timing signal described in section 3.3. Each gage record was read beginning at the nearest even millisecond before the first arrival at any gage on the structure involved. The trace deflection was read and converted into equivalent pressure for each millisecond during the diffraction phase or at odd half milliseconds where the record excursions indicated a need for this interpolation. After the first 30 to 60 msec, as indicated, the reading intervals were increased to 5 or 10 msec and continued throughout at least half of the positive phase.

Thereafter readings were taken at longer intervals to the maximum negative excursion. These tabulated data along with tracings of the original gage records are included in Appendix A.1/ The final pressure-time data as presented in this appendix are estimated to represent the actual pressure-time history at the gage to an accuracy of plus or minus 5 per cent or better. The absolute time measurements are calculated to be accurate to plus or minus 0.01 per cent plus or minus 0.25 msec. The original calibration data, corrected only for sensitivity changes as indicated by the calibrating signal ratio, are included for each channel in Appendix A.

When an average is taken of several gage channels to obtain the average pressure on a face of a structure the accuracy will probably be increased by this process, since none of the known causes of error have been found to be unidirectional. The same reasoning applies to the use of an average figure for side-on pressure calculations.

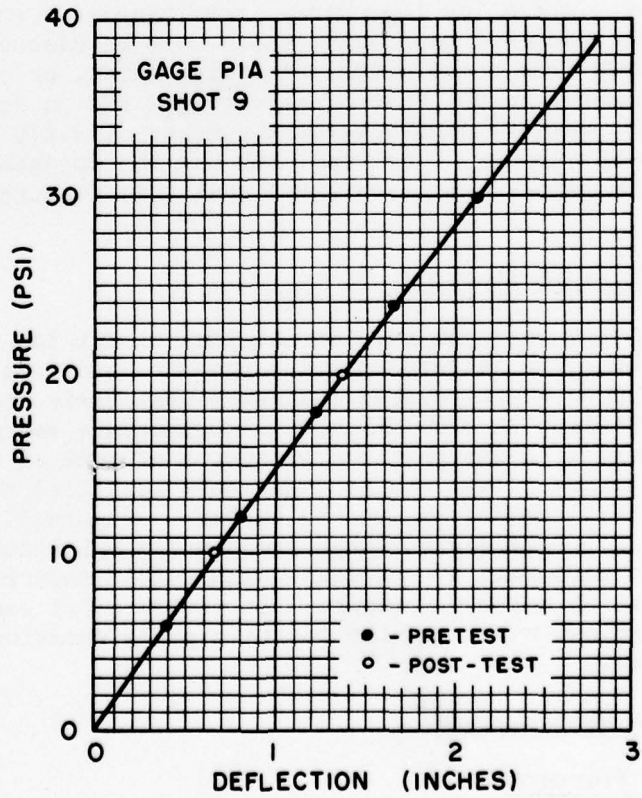


Fig. 4.1 Typical Calibration Curve

## CHAPTER 5

### RESULTS

#### 5.1 GENERAL

Of the total of 144 gage channels installed for this project on Shots 9 and 10, one channel failed to give a good readable record. This was gage BB on Shot 10, which appears to have been filled with sand or otherwise operating improperly, resulting in a record with a rounded wave form and low peak value which must be discounted. All records were free from undue noise, base line shift, or other disturbing influences. In the case of gage record P6A on Shot 9, there is an indicated pressure drop between the times of 3.679 sec and 3.686 sec which does not appear to be real, but has the appearance of an electrical disturbance. It is believed that this feature should be ignored.

#### 5.2 STRUCTURAL MEASUREMENTS

The 114 structural gage records obtained on the two shots are considered to be quite satisfactory for pressure analysis. A qualitative examination of these records indicates that their frequency resolution was sufficient to show all pertinent pressure variations in the diffraction phase with the possible exception of some of the gages installed on Structure 3.1-q. Where gages were installed adjacent to those of BRL the agreement is seen to be fair. Figure 5.1 compares the shape of the SRI records with the corresponding BRL records for those cases where the wave form was unusual. Table 5.1 compares the SRI and BRL measurements of maximum pressure, the pressure 0.1 sec after the arrival of the blast wave, and the positive phase duration for all corresponding gages.

#### 5.3 FREE-FIELD MEASUREMENTS

##### 5.3.1 Side-On Pressure

Tracings of the Shot 9 free-field pressure records are presented in Fig. 5.2.

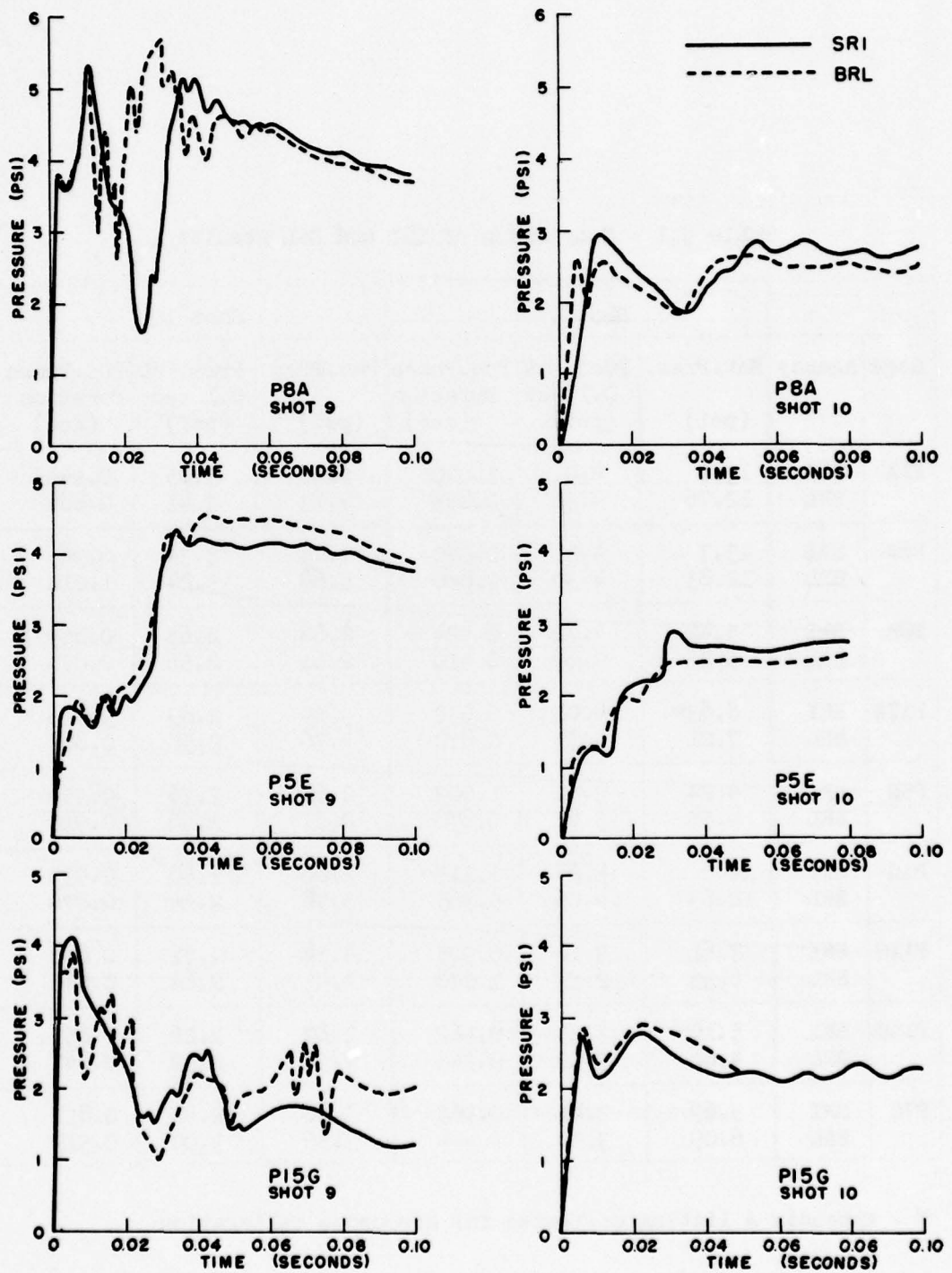


Fig. 5.1 Comparison of SRI and BRL Records

Table 5.1 - Comparison of SRI and BRL Results

|      |            | Shot 9             |                              |                                | Shot 10            |                              |                                |
|------|------------|--------------------|------------------------------|--------------------------------|--------------------|------------------------------|--------------------------------|
| Gage | Agency     | Max.Pres.<br>(psi) | Pres. at<br>0.1 sec<br>(psi) | Pos.Phase<br>Duration<br>(sec) | Max.Pres.<br>(psi) | Pres. at<br>0.1 sec<br>(psi) | Pos.Phase<br>Duration<br>(sec) |
| P1A  | SRI<br>BRL | 13.1<br>12.76      | 4.0<br>4.31                  | 1.070<br>0.853                 | 6.65<br>7.13       | 3.05<br>3.41                 | 0.945<br>0.884                 |
| P6A  | SRI<br>BRL | 13.7<br>12.83      | 4.3<br>4.30                  | 0.970<br>0.860                 | 7.25<br>6.68       | 3.34<br>3.24                 | 0.965<br>1.010                 |
| P8A  | SRI<br>BRL | 5.42<br>5.23       | 3.72<br>3.68                 | 0.924<br>0.910                 | 2.88<br>2.61       | 2.65<br>2.56                 | 0.869<br>0.876                 |
| P17A | SRI<br>BRL | 6.83*<br>7.21      | 4.00*<br>4.35                | 0.932<br>0.870                 | 3.59<br>3.36       | 2.85<br>2.58                 | 0.896<br>0.887                 |
| P5E  | SRI<br>BRL | 4.24<br>4.55       | 3.72<br>3.86                 | 1.003<br>0.878                 | 2.88<br>2.57       | 2.76<br>2.56                 | 0.959<br>0.916                 |
| P1G  | SRI<br>BRL | 12.2<br>12.63      | 4.2<br>4.06                  | 1.115<br>0.965                 | 5.88<br>5.78       | 2.40<br>2.94                 | 0.939<br>0.876                 |
| P11G | SRI<br>BRL | 7.61<br>6.93       | 3.16<br>2.97                 | 0.905<br>1.070                 | 4.54<br>4.43       | 2.71<br>2.64                 | 0.888<br>0.845                 |
| P15G | SRI<br>BRL | 5.10<br>4.86       | 3.25<br>3.02                 | 0.962<br>0.946                 | 2.82<br>2.94       | 2.26<br>2.32                 | 0.855<br>0.847                 |
| P7G  | SRI<br>BRL | 5.69<br>6.09       | 3.81<br>3.40                 | 0.969<br>-----                 | 3.18<br>3.56       | 2.44<br>3.00                 | 0.891<br>0.919                 |

\* - Appendix A listing corrected for erroneous calibration

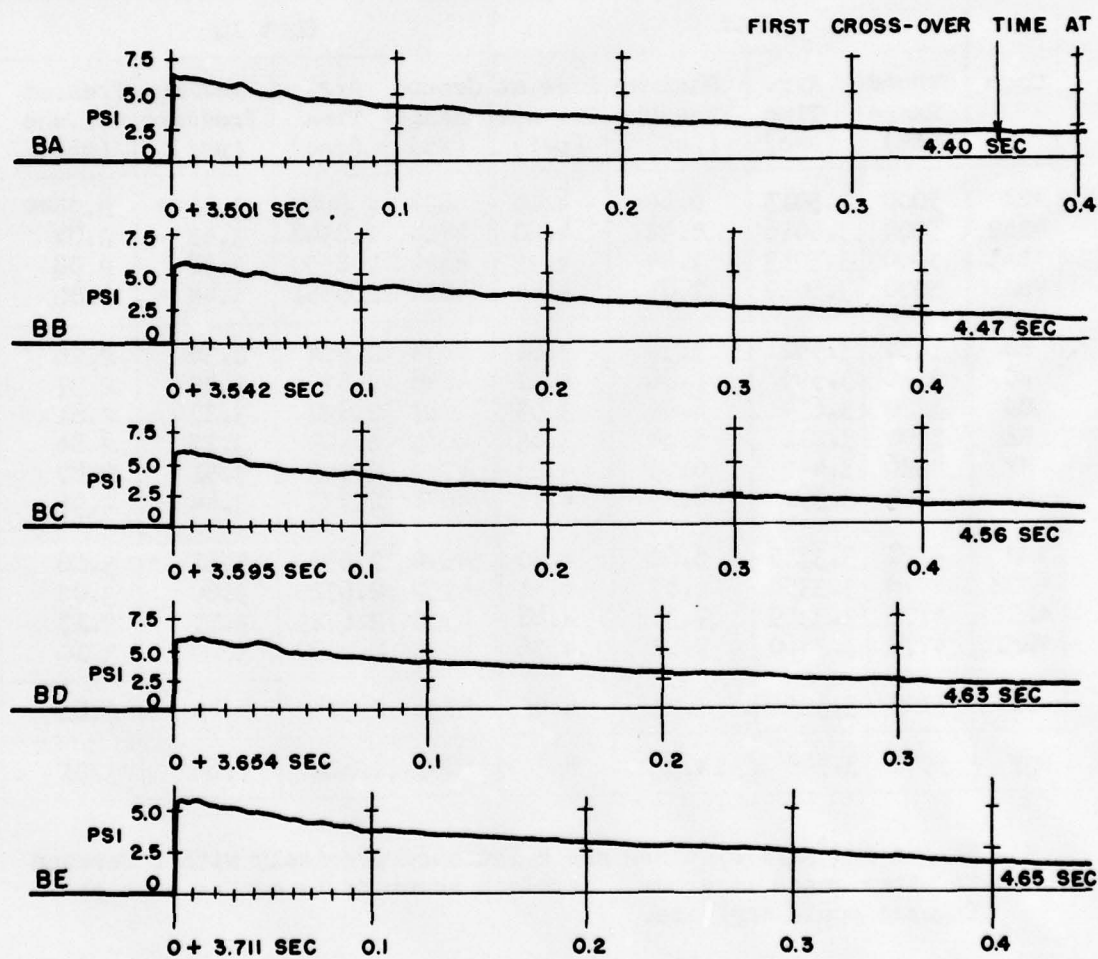


Fig. 5.2 Free-Field Records - Shot 9

Table 5.2 - Summary of Free-Field Measurements

| Gage  | Shot 9            |                 |                        |                        | Shot 10           |                 |                        |                        |
|-------|-------------------|-----------------|------------------------|------------------------|-------------------|-----------------|------------------------|------------------------|
|       | Ground Range (ft) | Arr. Time (sec) | Maximum Pressure (psi) | Pres. at 0.1 sec (psi) | Ground Range (ft) | Arr. Time (sec) | Maximum Pressure (psi) | Pres. at 0.1 sec (psi) |
| *BA   | 5000              | 3.5013          | 6.44                   | 4.05                   | 4824              | 2.8543          | 3.48**                 | 2.94**                 |
| *BA2  | 5000              | 3.5016          | 6.42                   | 4.20                   | 4824              | 2.8548          | 3.42                   | 2.84                   |
| *BA5  | 5000              | 3.5013          | 7.44                   | 4.35                   | 4824              | 2.8550          | 3.58                   | 2.88                   |
| *BA10 | 5000              | 3.5019          | 7.81                   | 4.64                   | 4824              | 2.8551          | 3.44                   | 2.86                   |
| BB    | 5058              | 3.542           | 5.59                   | 3.81                   | 4834              | 2.864           | 2.36                   | 2.26                   |
| BC    | 5130              | 3.595           | 5.86                   | 4.11                   | 4848              | 2.879           | 3.49                   | 2.97                   |
| BD    | 5220              | 3.654           | 6.05                   | 3.95                   | 4867              | 2.892           | 3.27                   | 2.81                   |
| BE    | 5301              | 3.711           | 5.64                   | 3.83                   | 4885              | 2.909           | 3.17                   | 2.84                   |
| BF    | 4926              | 3.445           | 6.69                   | 4.25                   | 4749              | 2.793           | 3.51                   | 2.87                   |
| BG    | 4852              | 3.390           | 6.29                   | 4.11                   | 4674              | 2.733           | 3.44                   | 2.96                   |
| *BH   | 4778              | 3.3355          | 6.62                   | 4.30                   | 4599              | 2.6729          | 3.67                   | 3.06                   |
| *BH2  | 4778              | 3.3358          | 6.87                   | 4.41                   | 4599              | 2.6729          | 3.66                   | 3.05                   |
| *BH5  | 4778              | 3.3359          | 7.35                   | 4.48                   | 4599              | 2.6729          | 3.77                   | 3.17                   |
| *BH10 | 4778              | 3.3360          | 7.62                   | 4.56                   | 4599              | 2.6732          | 3.69                   | 3.10                   |
| BI    | 5125              | 3.595           | 7.23                   | 4.09                   | 4891              | 2.914           | 4.49                   | 2.81                   |
| P3F   | 5071              | 3.548           | 14.9                   | 4.3                    | 4849              | 2.862           | 7.60                   | 3.01                   |

\* - Ranges and arrival times are calculated precisely with reference to other gages in array. Absolute accuracy is not as high as figures would indicate.

\*\* - Appendix A listing corrected for erroneous calibration.

Although the five basic free-field gages, BA through BE, were designed to be at the same radius (4900 ft) from ground zero, the wide deviation of true ground zero from nominal ground zero on Shot 9 resulted in a considerable difference in true ground range between these gages. As shown in Table 5.2, these ranges varied from 5000 to 5300 ft. This variation in range might be expected to cause a variation in peak pressure of slightly more than 6 per cent between the extreme gages. From Table 5.2 it will be observed that this variation was appreciably greater, approximately 14 per cent, and that the variation in pressure was not entirely orderly with range. When the pressures at equivalent later times in the positive phase duration are compared this variation becomes appreciably less. When corrected for range variations either of these figures is within the plus or minus 5 per cent accuracy expected of the system, but there is some reason to believe that these variations are real, indicating a partial asymmetry of the blast wave.

It may be desirable in the final analysis of the structural pressure data to reduce the side-on pressure gage readings to an idealized form eliminating the minor differences between individual records of side-on pressure. As a means for doing so, the individual gage records were compared with an idealized curve taken as

$$p = p_0 e^{-t/t_0} (1 - t/t_0), \quad (5.1)$$

where  $p$  is the idealized air pressure at time  $t$ ,  $p_0$  is the true maximum shock pressure, and  $t_0$  is the duration of the positive phase.

On Shot 9 it became apparent that the measurements depart noticeably from this equation. The records may, however, be divided into two parts each of which forms a satisfactory fit. The first 60 to 100 msec of each record fits an idealized curve with a  $t_0$  much smaller than the observed positive phase duration, while the next 400 msec of the record fit a similar curve with a  $t_0$  approximating the observed positive phase duration. This fitting was performed by plotting the records on log-log paper and comparing them with the idealized curve similarly plotted, as shown in Fig. 5.3. The results of these fitting processes are shown in Table 5.3. The average values for the five primary gages with the maximum deviation from these averages allow an evaluation of the process. It will be seen that the scatter of the curve fits for effective peak pressure ( $p_0$ ) is less than that of the maximum observed values.

The average side-on pressure curve obtained in this manner is shown in Fig. 5.4 and may be described as follows:

1. A peak pressure ( $p_0$ ) of 6.07 psi decays according to equation 5.1 ( $t_0 = 445$  msec) for approximately 85 msec, diverging to a curve of equation 5.1 ( $t_0 = 849$  msec) with an extrapolated  $p_0$  of 4.95 psi, continuing to approximately 450 msec. Beyond 450 msec, the slope decreases slightly and the curve crosses zero at 944 msec.

The importance of this deviation from the classical decay characteristics is not to be minimized; much attention has been given in loading tests to "scaling." The inclination in considerations of

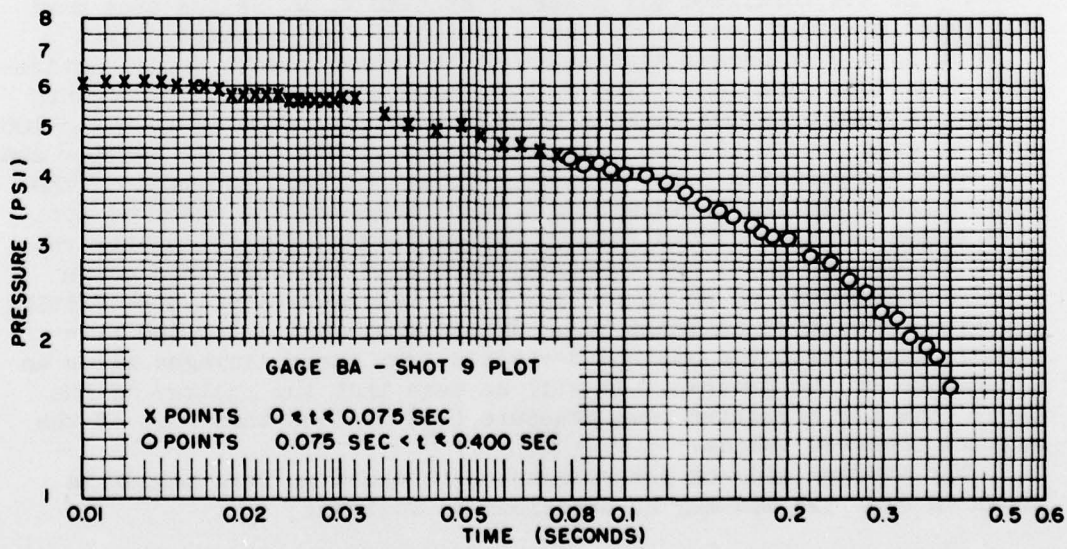
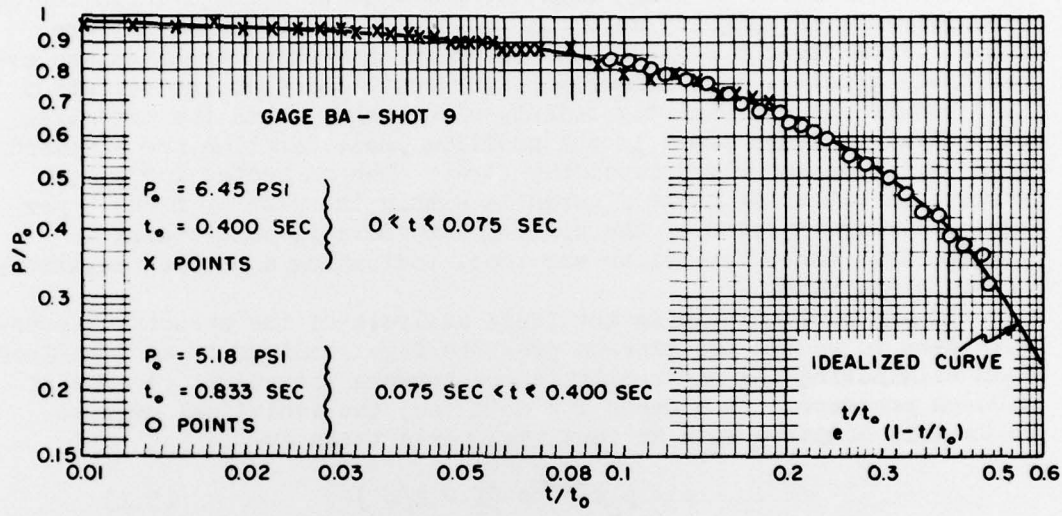


Fig. 5.3 Fitting Free-Field Records to Idealized Curve-Shot 9

Table 5.3 - Results of Curve Fittings

| Gage                            | Max.<br>Pres. | Shot 9                    |             |                                       |                             | Observed<br>$t_o$ (sec) | Ground<br>Range<br>(ft)               |
|---------------------------------|---------------|---------------------------|-------------|---------------------------------------|-----------------------------|-------------------------|---------------------------------------|
|                                 |               | $0 \leq t \leq 0.075$ sec | $t_o$ (sec) | Eff. Peak<br>Pres. ( $p_o$ )<br>(psi) | $0.075 \leq t \leq 0.4$ sec | $t_o$ (sec)             | Eff. Peak<br>Pres. ( $p_o$ )<br>(psi) |
| BA                              | 6.44          | 0.400                     | 6.45        | 833                                   | 5.18                        | 0.899                   | 5000                                  |
| BB                              | 5.59          | 0.475                     | 5.8         | 910                                   | 4.86                        | 0.939                   | 5058                                  |
| BC                              | 5.86          | 0.454                     | 6.00        | 833                                   | 4.95                        | 0.965                   | 5130                                  |
| BD                              | 6.05          | 0.400                     | 6.30        | 800                                   | 4.93                        | 0.976                   | 5220                                  |
| BE                              | 5.64          | 0.500                     | 5.8         | 870                                   | 4.81                        | 0.939                   | 5301                                  |
| Average<br>Max.Pos.<br>Dev. (%) | 5.82          | 0.445                     | 6.07        | 849                                   | 4.95                        | 0.944                   | 5150                                  |
| Max.Neg.<br>Dev. (%)            | 11            | 12                        | 6           | 7                                     | 3                           | 3.5                     | 3                                     |
| Max.Neg.<br>Dev. (%)            | 4             | 10                        | 4.5         | 6                                     | 5                           | 5                       | 3                                     |

$$\text{Ratio } (\frac{\text{eff.peak}}{\text{max.peak}}) = 1.04$$

| Gage                            | Max.<br>Pres. | $0 \leq t \leq 1.1$ sec |                                       | Observed<br>$t_o$ (sec) | Ground<br>Range<br>(ft) |
|---------------------------------|---------------|-------------------------|---------------------------------------|-------------------------|-------------------------|
|                                 |               | $t_o$ (sec)             | Eff. Peak<br>Pres. ( $p_o$ )<br>(psi) |                         |                         |
| BA                              | 3.48*         | 0.910                   | 3.47                                  | 0.876                   | 4824                    |
| BB                              | ----**        | ----                    | ----                                  | ----                    | ----                    |
| BC                              | 3.43          | 0.955                   | 3.50                                  | 0.872                   | 4848                    |
| BD                              | 3.27          | 0.955                   | 3.25                                  | 0.888                   | 4867                    |
| BE                              | 3.17          | 1.111                   | 3.25                                  | 0.862                   | 4885                    |
| Average<br>Max.Pos.<br>Dev. (%) | 3.32          | 0.983                   | 3.37                                  | 0.875                   | 4856                    |
| Max.Neg.<br>Dev. (%)            | 3             | 13                      | 4                                     | 1.5                     | 0.6                     |
| Max.Neg.<br>Dev. (%)            | 4.5           | 7                       | 4                                     | 1.5                     | 0.6                     |

$$\text{Ratio } (\frac{\text{eff.peak}}{\text{max.peak}}) = 1.02$$

\* - Appendix A listing corrected for erroneous calibration

\*\* - BB believed to be in error for Shot 10

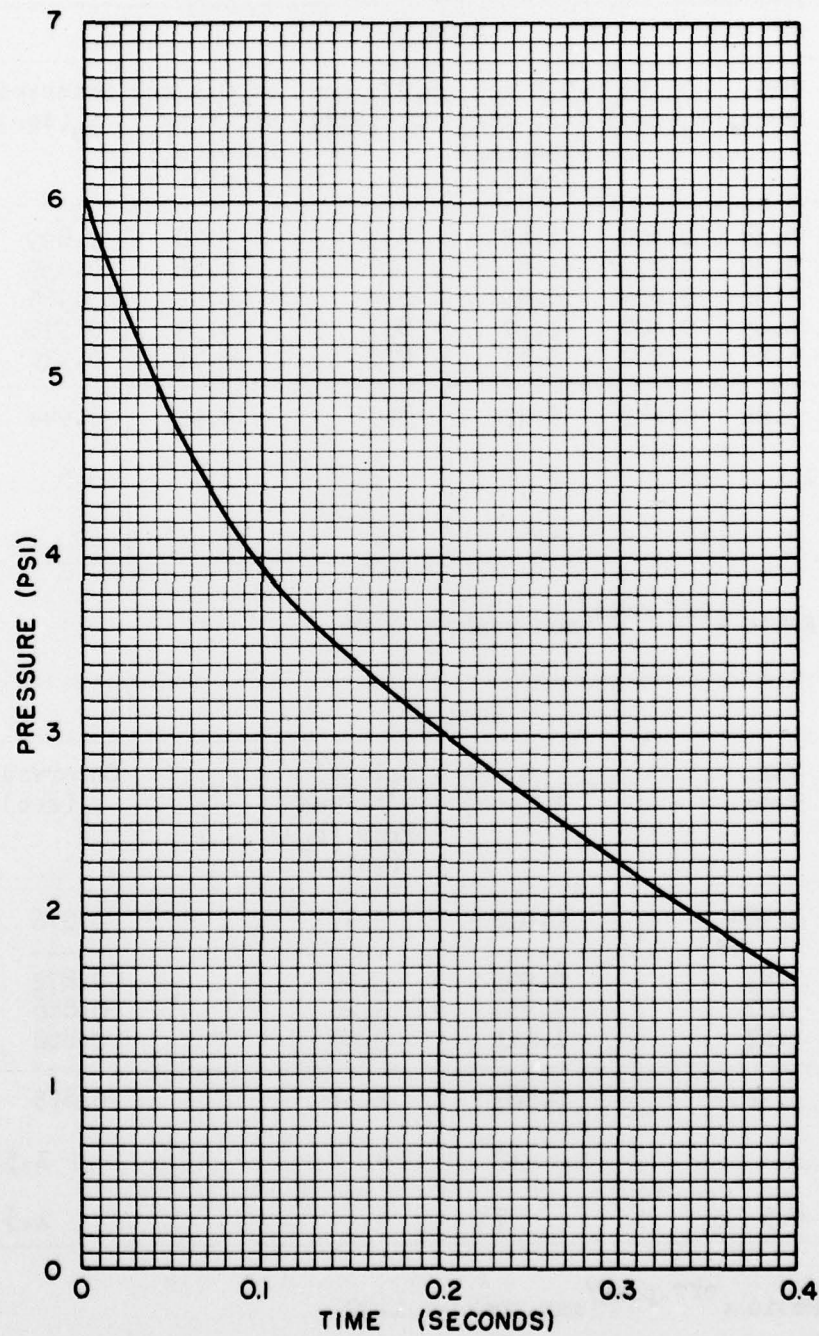


Fig. 5.4 Average Side-On Pressure Curve - Shot 9

scaling is to use the yield of the explosion as a measure of the scale. In this case, during the diffraction and other drag phases of the loading process the side-on pressure behaved as though it were derived from an explosion of approximately 1/8th the true yield of Shot 9. Comparisons with other tests should probably be made on this basis.

On Shot 10 the wave form was much more classic and a satisfactory fit of one curve was obtained. From Table 5.3 and Figs. 5.5 and 5.6 we find that the pressure decays from a peak of 3.37 psi according to equation 5.1 with a  $t_0$  of 983 msec. In the late portions of the curve the slope increases slightly, crossing zero at 875 msec (Fig. 5.7).

If these idealized curves are used as a basis of analysis of structural loading data, two refinements may be desirable:

1. In each case the curve represents the average pressure at the average ground range. A correction for true ground range may be applied to the pressure values. At this range the slope of the pressure-distance curve is very close to unity so that a proportional correction would suffice. This would result in a maximum correction of Structure 3.1a and 3.1g of about 3 per cent on Shot 9 and less than 3 per cent on Shot 10.

2. The observed peaks fall, on the average, 4 per cent lower than the  $p_0$  of the curve on Shot 9, 2 per cent lower on Shot 10. It is highly improbable that this is due to instrument characteristics. If this is to be considered, the first 10 msec of each curve should be "flat-topped."

### 5.3.2 Effect of Stabilization

Gage station BH (including BH2, BH5, and BH10) was placed outside of the stabilized area for purposes of comparison with BA, BA2, BA5, and BA10 which were within the stabilized area.

Two effects might be expected on the vertical shock wave from the unstabilized ground surface:

1. The peak pressure at and near the surface might be reduced.

2. The velocity near the surface might be reduced, causing the shock front to lean forward.

It was expected that if such effects were produced the stabilization would reduce them, resulting in a simpler analytical problem when the blast wave enveloped the 3.1 structures.

An examination of the data from the two vertical arrays (Table 5.2) shows no perceptible difference in the pressure gradient at the two arrays. On Shot 9 there is a slight indicated increase of pressure with height, but no change in this gradient at the two arrays. These readings may be discounted to some extent since the unfavorable angle of the baffles due to the displacement of ground zero makes the above-ground readings suspect. On Shot 10 the pressure vs. height readings

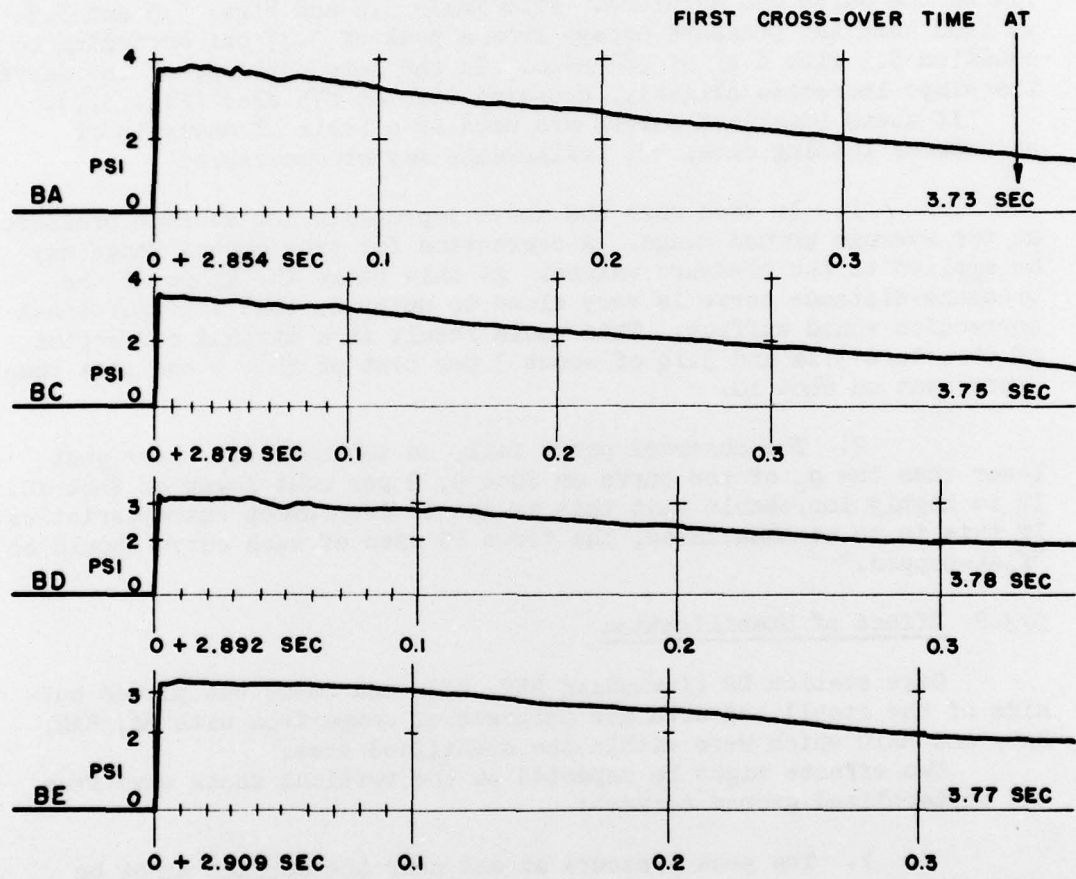


Fig. 5.5 Free-Field Records - Shot 10

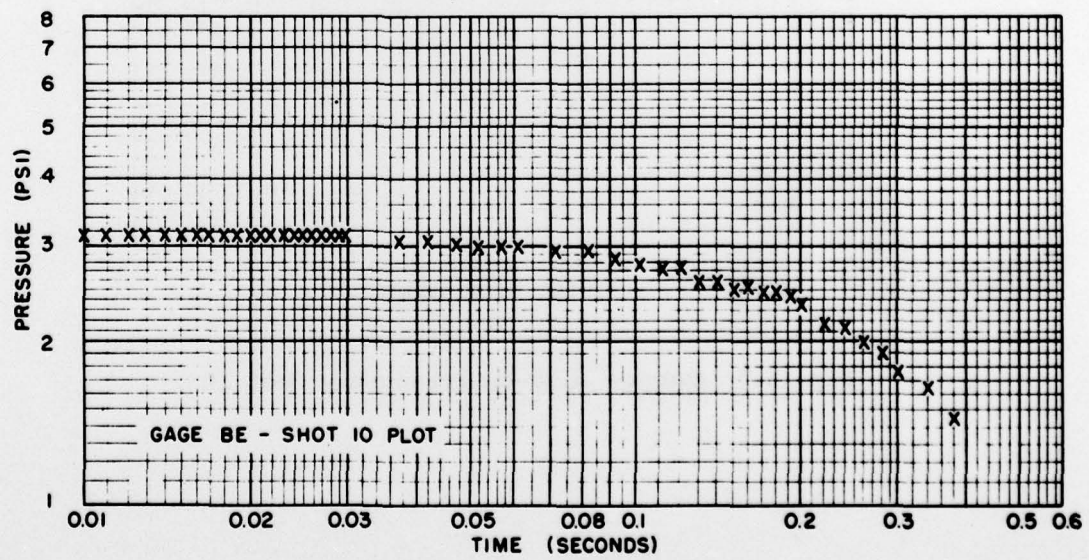
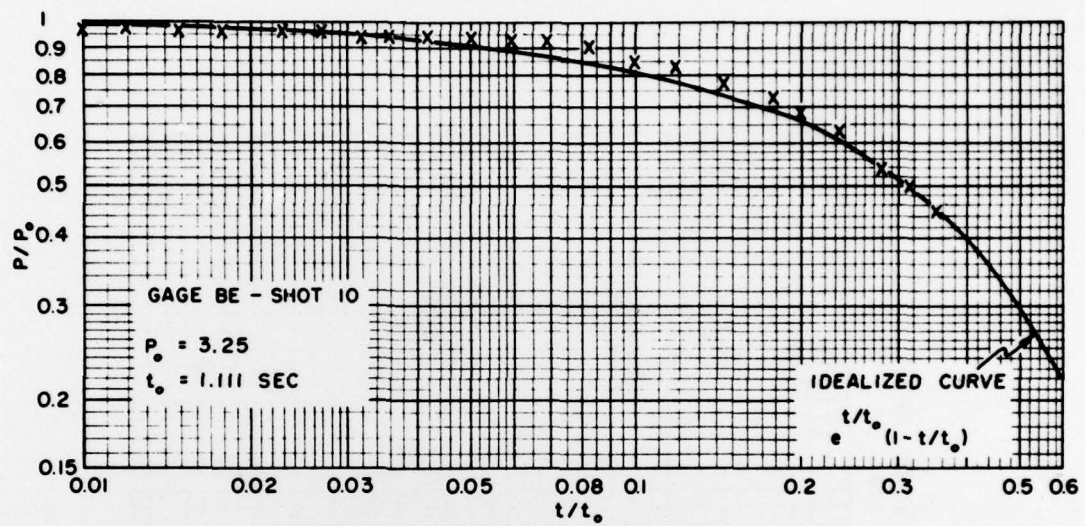


Fig. 5.6 Fitting Free-Field Records to Idealized Curve-Shot 10

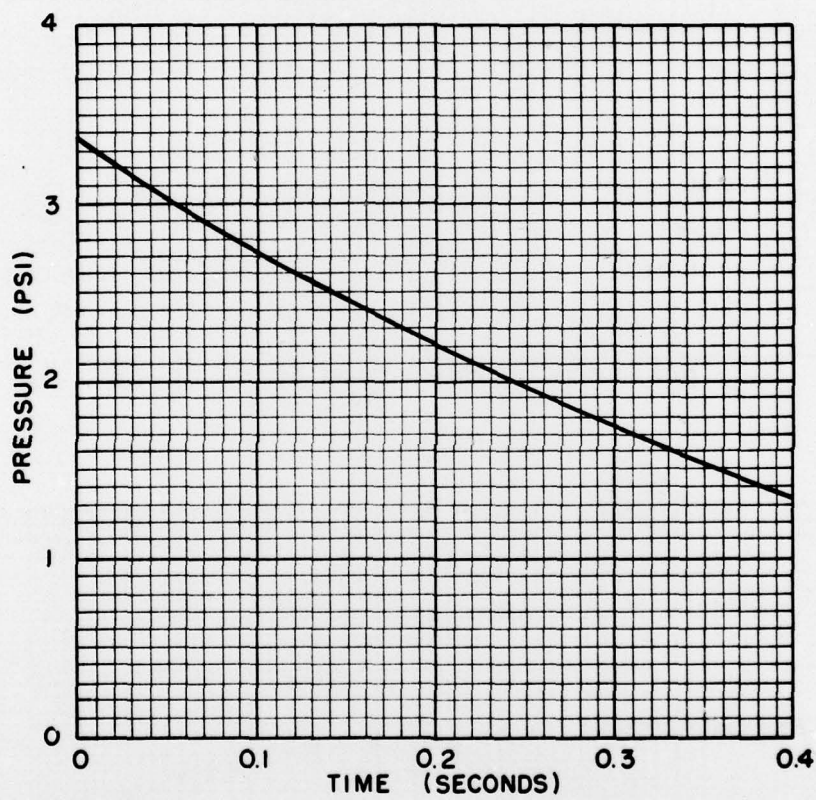


Fig. 5.7 Average Side-On Pressure - Shot 10

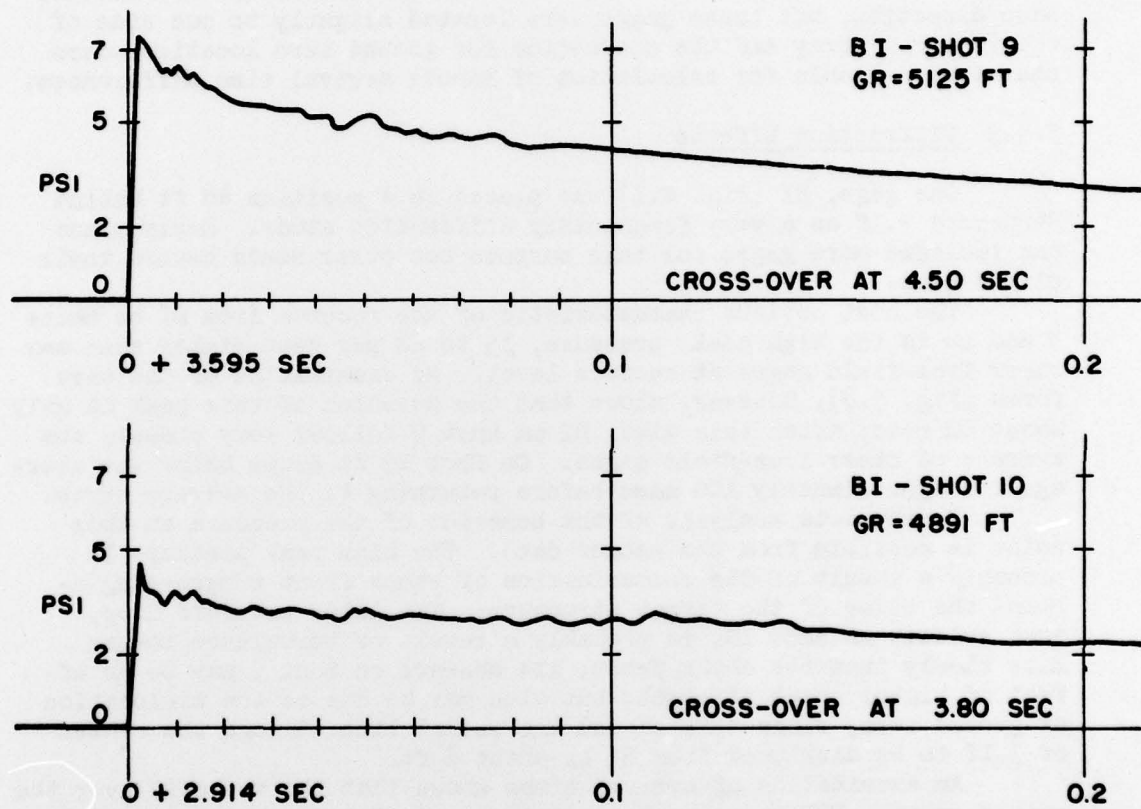


Fig. 5.8 Gage BI Records - Shots 9 and 10

are well within the scatter to be expected between gages.

A careful examination of the arrival times results in a similar conclusion. Comparing the 2-ft and 10-ft gages, we find approximately 0.25 msec difference in their arrival times at both stations on both shots. Contrary to what might be expected, the 2-ft arrival is the earlier, indicating a backward slope of the shock front, but the important observation is that this slope showed no indication of being changed by the stabilization. The surface level arrivals are in this same direction, but these gages were located slightly to one side of the vertical array and the correction for ground zero location makes them less reliable for calculation of minute arrival time differences.

### 5.3.3 Diffraction Effects

One gage, BI (Fig. 2.1) was placed in a position 48 ft behind Structure 3.1f as a very fragmentary diffraction study. Early plans had included more gages for this purpose but other needs caused their elimination.

The most obvious characteristic of the records from BI on Shots 9 and 10 is the high peak pressure, 15 to 20 per cent higher than any other free-field gages at surface level. An examination of the wave forms (Fig. 5.8), however, shows that the duration of this peak is only about 20 msec; after this time, BI on Shot 9 follows very closely the average of other free-field gages. On Shot 10 it drops below the average for approximately 100 msec before returning to the average curve.

No complete analysis of the behavior of the pressure at this point is possible from the meager data. The high peak pressure is probably a result of the recombination of shock front progressing around the sides of the target structure. The later pressure drop, most evident on Shot 10, is probably a result of turbulence moving more slowly than the shock front; its absence on Shot 9 may be an effect of higher shock strength, but also may be due to the mislocation of ground zero, since this caused the radial line through the center of 3.1f to be displaced from BI by about 8 ft.

An examination of arrival times shows that the velocity over the path from gage P3F to gage BI, a distance of 55.5 ft, was lower than the average velocity of the shock front. On Shot 9 this velocity was 1180 fps, on Shot 10, 1070 fps. These figures are compared with average shot velocities, of 1350 and 1240 fps respectively, of the undisturbed blast wave.

## CHAPTER 6

### CONCLUSIONS

#### 6.1 STRUCTURAL MEASUREMENTS

No conclusions are drawn from the results of the structural measurements since this is not the province of this project.

#### 6.2 FREE-FIELD MEASUREMENTS

The results of the side-on pressure measurements, although satisfactory showed sufficient variation to emphasize the importance of adequate instrumentation for determination of true side-on pressure in any loading tests. It is recommended that the planning for future tests give special consideration to this portion of such projects.

The study of the effects of stabilization leads to the definite conclusion that the stabilized surface had no measurably different effect on the blast wave than the natural surface in a distance of 200 ft. A less definite conclusion is that the unstabilized surface did not distort the wave front measurably in the Mach stem region.

The only conclusion which may be safely drawn from the meager diffraction data is that the shielding effect of a 3-dimensional structure of the general type of 3.1e is not completely negligible at a distance of four times the structure height. This does not infer that such shielding is useful in preventing damage; it may, in fact, increase the damage to glass and similar materials. This conclusion is essentially in accord with that reached by Sandia Corporation in a model study.<sup>8</sup>

## BIBLIOGRAPHY

1. Operation UPSHOT-KNOTHOLE, Project 3.28.3, Appendix A, Pressure Measurements on Structures, Stanford Research Institute. ~~SECRET-RESTRICTED DATA~~
2. Operation GREENHOUSE, Appendix I, Vol. I, Annex 3.3, Air Force Structures Program, Armour Final Results, WT-87. ~~CONFIDENTIAL-RESTRICTED DATA~~
3. Air Force Structures Program, Final Report, Planning Program for Air Force Structures Tests, Part IV, Loadings on Buildings and Equipment Shapes, AMC, July 1953. ~~SECRET~~
4. Operation TUMBLER, Final Summary Report, by H. Scoville et al, AFSWP, WT-514. ~~SECRET-RESTRICTED DATA~~
5. Operation UPSHOT-KNOTHOLE, Project 3.1, Tests on the Loading of Building and Equipment Shapes, by E. H. Wang and B. J. C'Brien, AMC, WT-721. ~~CONFIDENTIAL-RESTRICTED DATA~~
6. Operation TUMBLER, Project 1.2, Air Pressure vs Time, by V. Salmon, Stanford Research Institute, February 1953, WT-512. ~~SECRET-RESTRICTED DATA~~
7. Operation JANGLE, Project 1(9)a, Ground Acceleration, Ground and Air Pressures for Underground Test, by E. B. Doll, Stanford Research Institute, WT-380. ~~SECRET-RESTRICTED DATA~~
8. Shielding from Blast Waves by Parallel Structures, by M. L. Merritt, Sandia Corporation, AFSWP-224. ~~RESTRICTED~~

UNCLASSIFIED

## DISTRIBUTION

Military Distribution Categories 5-21 and 5-60

Copy

### ARMY ACTIVITIES

- 1 Asst. Chief of Staff, G-3, D/A, Washington 25, D.C.  
ATTN: Dep. CoFS, G-3 (RR&SW)
- 2 Asst. Chief of Staff, G-4, D/A, Washington 25, D.C.
- 3 Chief of Ordnance, D/A, Washington 25, D.C. ATTN:  
ORDTX-AR
- 4- 6 Chief Signal Officer, D/A, P&O Division, Washington  
25, D.C. ATTN: SIGOP
- 7 The Surgeon General, D/A, Washington 25, D.C. ATTN:  
Chief, R&D Division
- 8- 9 Chief Chemical Officer, D/A, Washington 25, D.C.
- 10 The Quartermaster General, CBR, Liaison Officer, Re-  
search and Development Div., D/A, Washington 25, D.C.
- 11- 15 Chief of Engineers, D/A, Washington 25, D.C. ATTN:  
ENGNB
- 16 Chief of Transportation, Military Planning and Intel-  
ligence Div., Washington 25, D.C.
- 17- 19 Chief, Army Field Forces, Ft. Monroe, Va.
- 20 President, Board #1, OCAFF, Ft. Bragg, N.C.
- 21 President, Board #2, OCAFF, Ft. Knox, Ky.
- 22 President, Board #3, OCAFF, Ft. Benning, Ga.
- 23 President, Board #4, OCAFF, Ft. Bliss, Tex.
- 24 Commanding General, U.S. Army Caribbean, Ft. Amador,  
C.Z. ATTN: Cml. Off.
- 25 Commander-in-Chief, European Command, APO 128, c/o PM,  
New York, N.Y.
- 26- 27 Commander-in-Chief, Far East Command, APO 500, c/o PM,  
San Francisco, Calif. ATTN: ACofS, J-3
- 28- 29 Commanding General, U.S. Army Europe, APO 403, c/o PM,  
New York, N.Y. ATTN: OPOT Div., Combat Dev. Br.
- 30- 31 Commandant, Command and General Staff College, Ft.  
Leavenworth, Kan. ATTN: ALLS(AS)
- 32 Commandant, The Artillery School, Ft. Sill, Okla.
- 33 Secretary, The AA&GM Branch, The Artillery School, Ft.  
Bliss, Tex. ATTN: Lt. Col. Albert D. Epley, Dept.  
of Tactics and Combined Arms
- 34 Commanding General, Medical Field Service School,  
Brooke Army Medical Center, Ft. Sam Houston, Tex.
- 35 Director, Special Weapons Development Office, Ft.  
Bliss, Tex. ATTN: Lt. Arthur Jaskierny
- 36 Commandant, Army Medical Service Graduate School,  
Walter Reed Army Medical Center, Washington 25, D.C.
- 37 Superintendent, U.S. Military Academy, West Point, N.Y.  
ATTN: Prof. of Ordnance
- 38 Commandant, Chemical Corps School, Chemical Corps  
Training Command, Ft. McClellan, Ala.
- 39 Commanding General, Research and Engineering Command,  
Army Chemical Center, Md. ATTN: Deputy for RW and  
Non-Toxic Material
- 40- 41 Commanding General, Aberdeen Proving Grounds, Md.  
(inner envelope) ATTN: RD Control Officer (for  
Director, Ballistics Research Laboratory)
- 42- 44 Commanding General, The Engineer Center, Ft. Belvoir,  
Va. ATTN: Asst. Commandant, Engineer School
- 45 Commanding Officer, Engineer Research and Development  
Laboratory, Ft. Belvoir, Va. ATTN: Chief, Technical  
Intelligence Branch
- 46 Commanding Officer, Picatinny Arsenal, Dover, N.J.  
ATTN: ORDBB-TK
- 47 Commanding Officer, Army Medical Research Laboratory,  
Ft. Knox, Ky.
- 48- 49 Commanding Officer, Chemical Corps Chemical and Radio-  
logical Laboratory, Army Chemical Center, Md. ATTN:  
Tech. Library
- 50 Commanding Officer, Transportation R&D Station, Ft.  
Eustis, Va.

Copy

- 51 Director, Technical Documents Center, Evans Signal  
Laboratory, Belmar, N.J.
- 52 Director, Waterways Experiment Station, PO Box 631,  
Vicksburg, Miss. ATTN: Library
- 53 Director, Armed Forces Institute of Pathology, 7th and  
Independence Avenue, S.W., Washington 25, D.C.
- 54 Director, Operations Research Office, Johns Hopkins  
University, 7100 Connecticut Ave., Chevy Chase, Md.  
ATTN: Library
- 55- 61 Technical Information Service, Oak Ridge, Tenn.  
(Surplus)

### NAVY ACTIVITIES

- 62- 63 Chief of Naval Operations, D/N, Washington 25, D.C.  
ATTN: OP-36
- 64 Chief of Naval Operations, D/N, Washington 25, D.C.  
ATTN: OP-374(OEG)
- 65 Director of Naval Intelligence, D/N, Washington 25,  
D.C. ATTN: OP-922V
- 66 Chief, Bureau of Medicine and Surgery, D/N, Washington  
25, D.C. ATTN: Special Weapons Defense Div.
- 67 Chief, Bureau of Ordnance, D/N, Washington 25, D.C.
- 68 Chief, Bureau of Ships, D/N, Washington 25, D.C. ATTN:  
Code 348
- 69 Chief, Bureau of Yards and Docks, D/N, Washington 25,  
D.C. ATTN: D-440
- 70 Chief, Bureau of Supplies and Accounts, D/N, Washing-  
ton 25, D.C.
- 71- 72 Chief, Bureau of Aeronautics, D/N, Washington 25, D.C.
- 73 Chief of Naval Research, Department of the Navy  
Washington 25, D.C. ATTN: LT(jg) F. McKee, USN
- 74 Commander-in-Chief, U.S. Pacific Fleet, Fleet Post  
Office, San Francisco, Calif.
- 75 Commander-in-Chief, U.S. Atlantic Fleet, U.S. Naval  
Base, Norfolk 11, Va.
- 76- 79 Commandant, U.S. Marine Corps, Washington 25, D.C.  
ATTN: Code AO3H
- 80 President, U.S. Naval War College, Newport, R.I.
- 81 Superintendent, U.S. Naval Postgraduate School,  
Monterey, Calif.
- 82 Commanding Officer, U.S. Naval Schools Command, U.S.  
Naval Station, Treasure Island, San Francisco,  
Calif.
- 83 Commanding Officer, U.S. Fleet Training Center, Naval  
Base, Norfolk 11, Va. ATTN: Special Weapons School
- 84- 85 Commanding Officer, U.S. Fleet Training Center, Naval  
Station, San Diego 36, Calif. ATTN: (SPWP School)
- 86 Commanding Officer, Air Development Squadron 5, VX-5,  
U.S. Naval Air Station, Moffett Field, Calif.
- 87 Commanding Officer, U.S. Naval Damage Control Training  
Center, Naval Base, Philadelphia 12, Pa. ATTN: ABC  
Defense Course
- 88 Commanding Officer, U.S. Naval Unit, Chemical Corps  
School, Army Chemical Training Center, Ft. McClellan,  
Ala.
- 89 Joint Landing Force Board, Marine Barracks, Camp  
Lejeune, N.C.
- 90 Commander, U.S. Naval Ordnance Laboratory, Silver  
Spring 19, Md. ATTN: EE
- 91 Commander, U.S. Naval Ordnance Laboratory, Silver  
Spring 19, Md. ATTN: EE
- 92 Commander, U.S. Naval Ordnance Laboratory, Silver  
Spring 19, Md. ATTN: R
- 93 Commander, U.S. Naval Ordnance Test Station  
China Lake, Calif.

UNCLASSIFIED

CONFIDENTIAL RESTRICTED DATA

~~CONFIDENTIAL~~

Copy

94 Officer-in-Charge, U.S. Naval Civil Engineering Res. and Evaluation Lab., U.S. Naval Construction Battalion Center, Port Hueneme, Calif. ATTN: Code 753  
95 Commanding Officer, U.S. Naval Medical Research Inst., National Naval Medical Center, Bethesda 14, Md.  
96 Director, U.S. Naval Research Laboratory, Washington 25, D.C. ATTN: Code 2029  
97 Commanding Officer and Director, U.S. Navy Electronics Laboratory, San Diego 52, Calif. ATTN: Code 4223  
98- 99 Commanding Officer, U.S. Naval Radiological Defense Laboratory, San Francisco 24, Calif. ATTN: Technical Information Division  
100-101 Commanding Officer and Director, David W. Taylor Model Basin, Washington 7, D.C. ATTN: Library  
102 Commander, U.S. Naval Air Development Center, Johnsville, Pa.  
103 Director, Office of Naval Research Branch Office, 1000 Geary St., San Francisco, Calif.  
104-110 Technical Information Service, Oak Ridge, Tenn.  
(Surplus)

AIR FORCE ACTIVITIES

111 Asst. for Atomic Energy, Headquarters, USAF, Washington 25, D.C. ATTN: DCS/O  
112 Director of Operations, Headquarters, USAF, Washington 25, D.C. ATTN: Operations Analysis  
113 Director of Plans, Headquarters, USAF, Washington 25, D.C. ATTN: War Plans Div.  
114 Director of Research and Development, Headquarters, USAF, Washington 25, D.C. ATTN: Combat Components Div.  
115-116 Director of Intelligence, Headquarters, USAF, Washington 25, D.C. ATTN: AFQIN-1B2  
117 The Surgeon General, Headquarters, USAF, Washington 25, D.C. ATTN: Bio. Def. Br., Pre. Med. Div.  
118 Asst. Chief of Staff, Intelligence, Headquarters, U.S. Air Forces Europe, APO 633, c/o PM, New York, N.Y.  
ATTN: Air Intelligence Branch  
119 Commander, 497th Reconnaissance Technical Squadron (Augmented), APO 633, c/o PM, New York, N.Y.  
120 Commander, Far East Air Forces, APO 925, c/o PM, San Francisco, Calif.  
121 Commander, Strategic Air Command, Offutt Air Force Base, Omaha, Nebraska. ATTN: Special Weapons Branch, Inspection Div., Inspector General  
122 Commander, Tactical Air Command, Langley AFB, Va.  
ATTN: Documents Security Branch  
123 Commander, Air Defense Command, Ent AFB, Colo.  
124-125 Commander, Air Materiel Command, Wright-Patterson AFB, Dayton, O. ATTN: MCAIDS  
126 Commander, Air Training Command, Scott AFB, Belleville, Ill. ATTN: DCS/O GTP  
127 Commander, Air Research and Development Command, PO Box 1395, Baltimore, Md. ATTN: RDRN  
128 Commander, Air Proving Ground Command, Eglin AFB, Fla. ATTN: AG/TRB  
129-130 Commander, Air University, Maxwell AFB, Ala.  
131-138 Commander, Flying Training Air Force, Waco, Tex.  
ATTN: Director of Observer Training  
139 Commander, Crew Training Air Force, Randolph Field, Tex. ATTN: 2OTS, DCS/O  
140 Commander, Headquarters, Technical Training Air Force, Gulfport, Miss. ATTN: TA&D

Copy

141-142 Commandant, Air Force School of Aviation Medicine, Randolph AFB, Tex.  
143-148 Commander, Wright Air Development Center, Wright-Patterson AFB, Dayton, O. ATTN: WCOESP  
149 Commander, Air Force Cambridge Research Center, 230 Albany Street, Cambridge 39, Mass. ATTN: CRW, Atomic Warfare Directorate  
150 Commander, Air Force Cambridge Research Center, 230 Albany Street, Cambridge 39, Mass. ATTN: CRST-2  
151-153 Commander, Air Force Special Weapons Center, Kirtland AFB, N. Mex. ATTN: Library  
154 Commandant, USAF Institute of Technology, Wright-Patterson AFB, Dayton, O. ATTN: Resident College  
155 Commander, Lowry AFB, Denver, Colo. ATTN: Department of Armament Training  
156 Commander, 1009th Special Weapons Squadron, Headquarters, USAF, Washington 25, D.C.  
157-158 The RAND Corporation, 1700 Main Street, Santa Monica, Calif. ATTN: Nuclear Energy Division  
159-165 Technical Information Service, Oak Ridge, Tenn.  
(Surplus)

OTHER DEPARTMENT OF DEFENSE ACTIVITIES

166 Asst. Secretary of Defense, Research and Development, D/D, Washington 25, D.C.  
167 U.S. National Military Representative, Headquarters, SHAPE, APO 55, c/o PM, New York, N.Y. ATTN: Col. J. P. Healy  
168 Director, Weapons Systems Evaluation Group, OSD, Rm 2E1006, Pentagon, Washington 25, D.C.  
169 Armed Services Explosives Safety Board, D/D, Building T-7, Gravelly Point, Washington 25, D.C.  
170 Commander, Armed Forces Staff College, Norfolk 11, Va. ATTN: Secretary  
171-176 Commanding General, Field Command, Armed Forces Special Weapons Project, PO Box 5100, Albuquerque, N. Mex.  
177-178 Commanding General, Field Command, Armed Forces, Special Weapons Project, PO Box 5100, Albuquerque, N. Mex.  
ATTN: Technical Training Group  
179-187 Chief, Armed Forces Special Weapons Project, Washington 25, D.C.  
188-194 Technical Information Service, Oak Ridge, Tenn.  
(Surplus)

ATOMIC ENERGY COMMISSION ACTIVITIES

195-197 U.S. Atomic Energy Commission, Classified Technical Library, 1901 Constitution Ave., Washington 25, D.C.  
ATTN: Mrs. J. M. O'Leary (For DMA)  
198-200 Los Alamos Scientific Laboratory, Report Library, PO Box 1663, Los Alamos, N. Mex. ATTN: Helen Redman  
201-206 Sandia Corporation, Classified Document Division, Sandia Base, Albuquerque, N. Mex. ATTN: Martin Lucero  
207-208 University of California Radiation Laboratory, PO Box 808, Livermore, Calif. ATTN: Margaret Edlund  
209 Weapon Data Section, Technical Information Service, Oak Ridge, Tenn.  
210-270 Technical Information Service, Oak Ridge, Tenn.  
(Surplus)

~~UNCLASSIFIED~~

~~CONFIDENTIAL~~  
~~RESTRICTED DATA~~



**Defense Special Weapons Agency**  
6801 Telegraph Road  
Alexandria, Virginia 22310-3398

OPSSI

MAY 8 1998

**MEMORANDUM FOR DISTRIBUTION**

**SUBJECT: Declassification Review of Operation UPSHOT-KNOTHOLE Test Reports**

The following 90 reports concerning the atmospheric nuclear tests conducted during Operation UPSHOT-KNOTHOLE in 1953 have been declassified and cleared for open publication/public release:

WT-702, WT-703, WT-705, WT-709 thru WT-711, WT-713 thru WT-719, WT-721 thru WT-742, WT-744 thru WT-746, WT-749 thru WT-755, WT-757 thru WT-761, WT-763, WT-764, WT-766 thru WT-781, WT-784 thru WT-787, WT-789, WT-790, WT-792 thru WT-796, WT-798, WT-801, WT-805, WT-808, WT-809, WT-811, WT-812, WT-814, WT-817, WT-820, and WT-822

An additional 6 WTs from UPSHOT-KNOTHOLE have been re-issued with deletions and are identified with an "EX" after the WT number. These reissued versions are unclassified and approved for open publication. They are:

WT-743, WT-747, WT-802, WT-810, WT-825, and WT-828

This memorandum supersedes the Defense Special Weapons Agency, OPSSI memorandum same subject dated June 11, 1997 and may be cited as the authority to declassify copies of any of the reports listed in the first paragraph above.

*Rita Metro*  
RITA M. METRO  
Chief, Information Security

**DISTRIBUTION**

See Attached